



## Simple strategy for single-chain fragment antibody-conjugated probe construction



Chen Xu<sup>a</sup>, Xiang Chen<sup>b</sup>, Mingjuan Yang<sup>b</sup>, Xiaopeng Yuan<sup>c</sup>, Aizhi Zhao<sup>b,\*\*</sup>, Hujing Bao<sup>d,\*</sup>

<sup>a</sup> Laboratory Science Department, Tianjin 4th Central Hospital, Tianjin, China, Abramson Cancer Center, Perelman School of Medicine, University of Pennsylvania, Philadelphia, PA, USA

<sup>b</sup> Abramson Cancer Center, Perelman School of Medicine, University of Pennsylvania, Philadelphia, PA, USA

<sup>c</sup> Zhujiang Hospital, Southern Medical University, Guangzhou, China, Abramson Cancer Center, Perelman School of Medicine, University of Pennsylvania, Philadelphia, PA, USA

<sup>d</sup> Integrative Medical Diagnosis Laboratory, Tianjin Nankai Hospital, Room 441, 4th Floor of Outpatient Building, Changjiang Road #6, Nankai District, Tianjin, 300100, China

### ARTICLE INFO

#### Keywords:

scFv  
SPIO  
ICG  
Tumor diagnosis  
Molecular imaging

### ABSTRACT

**Aims:** A combination of biomarker and instrument technology diagnosis methods, especially antigen-targeted imaging methods, is required to increase the accuracy of the diagnosis of cancer. Currently, the targeting efficiency is limited by the conjugation methods used for the conjugation of antibodies and imaging materials. Here, a simple strategy for the conjugation of a probe and a single-chain fragment antibody (scFv) that does not change the characteristics of the antibody was shown.

**Main methods:** An ScFv was conjugated with superparamagnetic iron oxide (SPIO) or indocyanine green (ICG) via a linker by utilizing the reaction between cysteine and maleimide. The characterization of the probe was performed by flow cytometry, confocal imaging, optical imaging and magnetic resonance imaging (MRI).

**Key findings:** After conjugation, the scFv retained high affinity, antigen specificity, and strong internalization ability. The application of the conjugated probe was also confirmed by optical imaging and MRI.

**Significance:** The proposed strategy provides a simple method for the production of high efficiency antigen-targeted imaging probes for tumor diagnosis.

### 1. Introduction

The diagnosis of tumors currently relies on the detection of serum tumor-associated antigens (TAAs) and imaging detection, including magnetic resonance imaging (MRI), ultrasound testing and other imaging tests. Because of the nonspecificity of TAAs, tumor marker screening alone is insufficient for the accurate diagnosis of tumors. In addition, good training and adequate experience are very important for imaging diagnostic accuracy. Therefore, new diagnostic methods, especially antigen-targeted imaging methods, are required to increase the accuracy of tumor diagnosis. In fact, the future of tumor diagnosis is likely to utilize a combination of biomarkers and instrument technology, known as “molecular imaging”. Because most new imaging methods are based on an antibody-specific reaction with a tumor antigen, these methods are also called “immunoscopes”. Although many monoclonal antibody (mAb)-based MRI probes or fluorescence probes have been developed, their actual tumor penetration efficiency is

limited by their size (approximately 150 kDa for mAbs). Macromolecules, such as mAbs, are often inefficient at penetrating through a tumor due to high interstitial pressure and dense fibrosis [1,2]. Single-chain fragment (scFv) antibodies consist of only one variable region of the heavy chain ( $V_H$ ) and one variable region of the light chain ( $V_L$ ) and therefore are much smaller in size than mAbs. Because of their reduced size, scFv antibody derivatives have favorable characteristics, especially in terms of tumor penetration. Moreover, the off-target effects on Fc receptor (FCR)-positive cells are decreased by the absence of the Fc region [3–6]. Additionally, due to their small size, scFvs have characteristics (affinity, specificity and internalization ability) that could be significantly altered by the methods used for probe conjugation, which could affect the targeting efficiency of the antigen-targeted probe for cancer diagnosis and even for immunotherapy.

By introducing one free cysteine into an scFv, as was already mentioned in the paper by Backmann et al. (2005), scFvs were

\* Corresponding author.

\*\* Corresponding author.

E-mail addresses: [Aizhizhao@gmail.com](mailto:Aizhizhao@gmail.com) (A. Zhao), [kris\\_10713@126.com](mailto:kris_10713@126.com) (H. Bao).

<https://doi.org/10.1016/j.lfs.2019.117052>

Received 15 July 2019; Received in revised form 29 October 2019; Accepted 7 November 2019

Available online 13 November 2019

0024-3205/ © 2019 Elsevier Inc. All rights reserved.

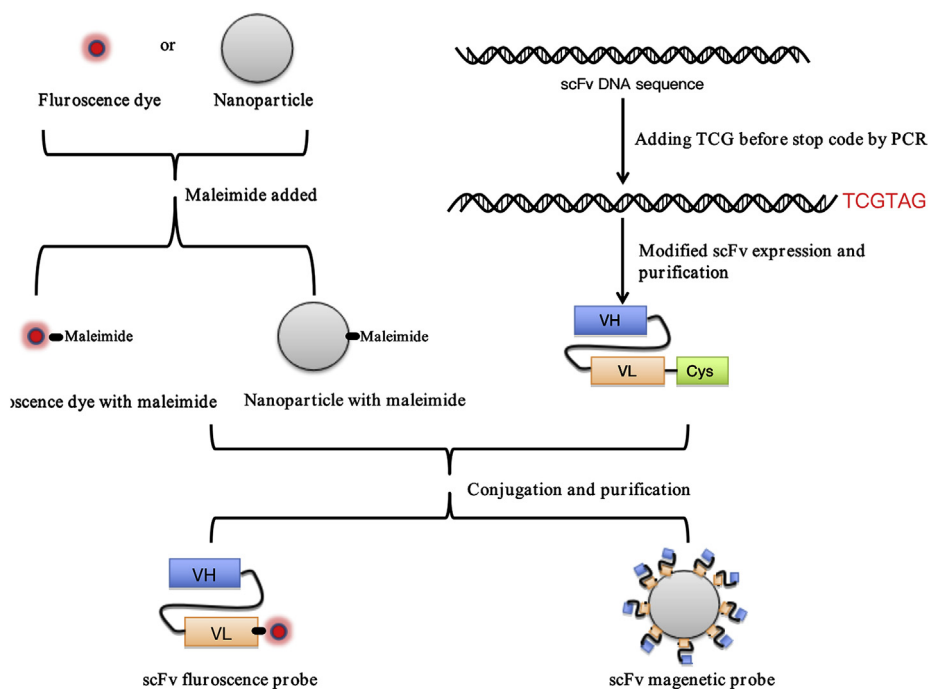


Fig. 1. The illustration for the conjugation between scFv and the probe.

conjugated to an Au-precoated plate to create immunosensor arrays to detect proteins *in vitro* [7]. However, in our strategy, not only is a free cysteine introduced into the scFv sequence, but different chemical reactions and linkers are utilized during conjugation to the SPIO or ICG dye to reduce the effects on the characteristics of the scFv. Herein, we reported new simple strategies for scFv-conjugated molecular imaging probes that have little effect on the affinity, specificity and internalization ability during tumor-targeted diagnosis or immunotherapy (Fig. 1). The scFv-based antigen-targeted probe was constructed by the simple conjugation of a cysteine in the C-terminal of the scFv with maleimide probes at room temperature for 2 h or at 4 °C overnight. Ovarian cancer (OC) is a major cause of cancer-related deaths in women in the US [8] and has a very high mortality rate in China. Patients with OC have a very poor prognosis, mainly due to poor early diagnosis methods. Tumor endothelium marker 1 (TEM1) is a novel surface marker for many solid tumors, including OC. Our group has successfully isolated and characterized the first fully human anti-TEM1 scFv (scFv78) [9,10]. In this paper, anti-TEM1 scFv was used for the evaluation of strategies for nanoparticle (SPIO) conjugation or fluorescence dye (ICG) conjugation. All characterizations and measurements were performed in OC cell lines.

## 2. Materials and methods

### 2.1. scFv purification

The scFv plasmid was transformed into *E. coli*. After the clones formed, a single clone was transferred into 5 ml Luria-Bertani (LB) culture media from the plate and incubated at 37 °C overnight. The next day, the bacteria were seeded into a new 500 ml LB culture at a 1:100 dilution ratio, which was cultured until the OD450 reached 0.6 (approximately 2 h). IPTG (Sigma-Aldrich, I6758) at a final concentration of 1 mM was added to the culture to induce scFv expression, and the culture was incubated for another 2 h. After IPTG induction, the bacteria were washed with 40 ml equilibrium buffer (EQ buffer: 135 mM NaCl, 2.7 mM KCl, 1.5 mM KH<sub>2</sub>PO<sub>4</sub>, 8 mM K<sub>2</sub>HPO<sub>4</sub> and 8 M urea, pH 7.2). Then, the scFv was purified by Ni-NTA agarose (ThermoFisher, R90115) under denaturing conditions using 8 M urea and then

renatured by dialysis in 5 L PBS three times overnight. After renaturation, the scFv was concentrated to 1 mg/ml in a concentration tube with a 10 KD cutoff (ThermoFisher 88535). The purity of the scFv was detected by SDS-PAGE, and the affinity was measured by ELISA.

### 2.2. Construction and characterization of SPIO-78C

**SPIO-78C construction.** First, 100 µl (4.8 mg/ml in DI water) Sulfo-SMCC linker (Thermo, 92921-24-9) was incubated with SPIO (500 µg, 3.5 mg/ml) with gentle shaking for 30 min at room temperature, after which the conjugation solution was gently loaded into a desalting column (Thermo, 89889) and spun down at 1000 g for 2 min to remove the excess crosslinker. Second, 400 µg scFv (78C) was conjugated with the SPIO linker by mixing and gentle shaking for 2 h at room temperature or at 4 °C overnight. After conjugation, 100 µl of 20 mM freshly prepared cysteine solution (Sigma, MKBG4156V) was added to block the free maleimide on the nanoparticles with gentle shaking for 1 h at room temperature. Finally, SPIO-78C was purified using magnetic columns (MACS, 130-042-401) and concentrated in a concentration tube with a 100 KD cutoff (ThermoFisher 88537). DLS was used to measure the size of SPIO, and a minispacer was used to measure R2. ELISA and FACS were used for the affinity, specificity and internalization testing.

**Confocal microscopy for internalization evaluation.** The MS1 and MS1-TEM1 cells were seeded on coverslips in precoated 24-well plates and then incubated overnight at 37 °C. After incubation with SPIO-78C, anti-His monoclonal antibody (ThermoFisher MAI-21315) and anti-mouse Fc-APC (ThermoFisher, 31982) overnight at 4 °C, the antibody mixture was added to each well, and the cells were then incubated for 2 h at 37 °C or 4 °C. After washing twice with PBS, 1% formaldehyde was used to fix the cells, and then 5% BSA was used for blocking. DAPI (Invitrogen, D3571) at a final concentration of 0.1 µg/ml was used for nuclear staining, and DIOc18(3) (Invitrogen D275) at a final concentration of 10 µg/ml was used for membrane staining.

**Cell pellets for MRI imaging testing.** MS1 or MS1-TEM1 cells were detached with Versene solution, and 4x10<sup>6</sup> cells were incubated with 80 µl unlabeled NPs, SPIO-78C (300 µg Fe/200 µl) or scFv only for 2 h at 4 °C. After two washes, the cell pellets were transferred to MRI plates and then subjected to MRI imaging. The experiment was conducted

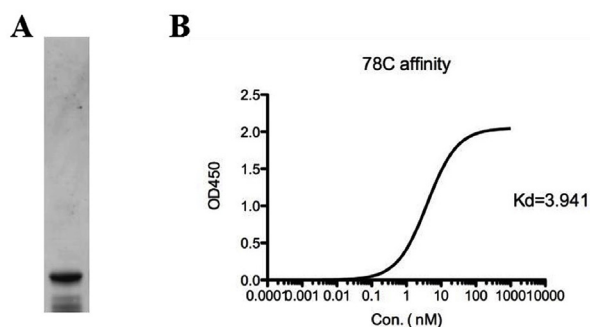


Fig. 2. Construction and characterization of the cysteine-conjugated anti-TEM1 scFv (78C). A. 78C purification measurement by SDS-PAGE. B. The affinity of 78C was detected by cell ELISA.

twice, and the statistical analysis was performed with one-way ANOVA and Tukey's multiple comparison test.

### 2.3. Construction and characterization of the fluorescent dye-conjugated scFv

First, 2 mg ICG-NHS (InTrace 004-901, 10 mg package) was used for conjugation along with 1 mg NH<sub>2</sub>-PEG-MAL (Creative PEGworks, PHB-943, 10K, 100 mg package) by gentle mixing and incubation at room temperature for 2 h. The free ICG-NHS was removed by a desalting column (Thermo, 89889). Then, 500 µg 78C (1 mg/ml) was conjugated with ICG-PEG with shaking at room temperature for 2 h. Finally, 78C-ICG was purified and concentrated in a concentration tube with a 10 KD cutoff (ThermoFisher 88535). The affinity of 78C-ICG was evaluated by ELISA, and the purity was detected by optical imaging. ELISA and FACS were used for the affinity, specificity and internalization testing.

### 2.4. ELISA

After using 50 µl 2% gelatin to precoat a 96-well plate at 37 °C for 1 h, MS1 or MS1-TEM1 cells were seeded into each well at a density of approximately 10<sup>4</sup>-10<sup>5</sup> cells/well (200 µl/well) and incubated overnight at 37 °C. On the next day, appropriate dilutions of antibodies were added to each well, which were incubated at 4 °C for 1 h. After washing three times, the secondary antibody was added to each well, and the cells were incubated for another hr. Finally, 100 µl/well TMB was added, and the cells were incubated for 30 min. Then, 100 µl/well stop solution was added to stop the reaction.

### 2.5. Flow cytometric testing

The cells were digested by using 6 ml Versene solution (Versene, 0.02%, in 1.37 M NaCl, 26.8 mM Na<sub>2</sub>HPO<sub>4</sub>, 14.7 mM KH<sub>2</sub>PO<sub>4</sub>, 5.4 mM disodium EDTA, and 0.2% D-glucose with phenol red) with incubation at 37 °C for approximately 10 min, after which the reaction was stopped by adding the same volume of cell culture medium into the flask.

After the cells were harvested, an appropriate volume of FACS buffer (0.5% BSA (2.5 g) and 2 mM EDTA in 500 ml buffer) was added into a 50 ml tube and gently mixed well, after which it was aliquoted into an appropriate number of FACS tubes. After washing the cells with FACS buffer, appropriate concentration antibody (50 mM SPIO-78C, 50 nM ICG-78C or scFv only) was added to the tube, which was incubated for 1 h at 4 °C (to avoid internalization) or 37 °C (to induce internalization). Then, 100 µl anti-His antibody and anti-mouse Fc-APC were added to each tube. After adding 300 µl of denatured probe to each tube, flow cytometry was conducted to measure the fluorescence of the cells.

## 3. Results

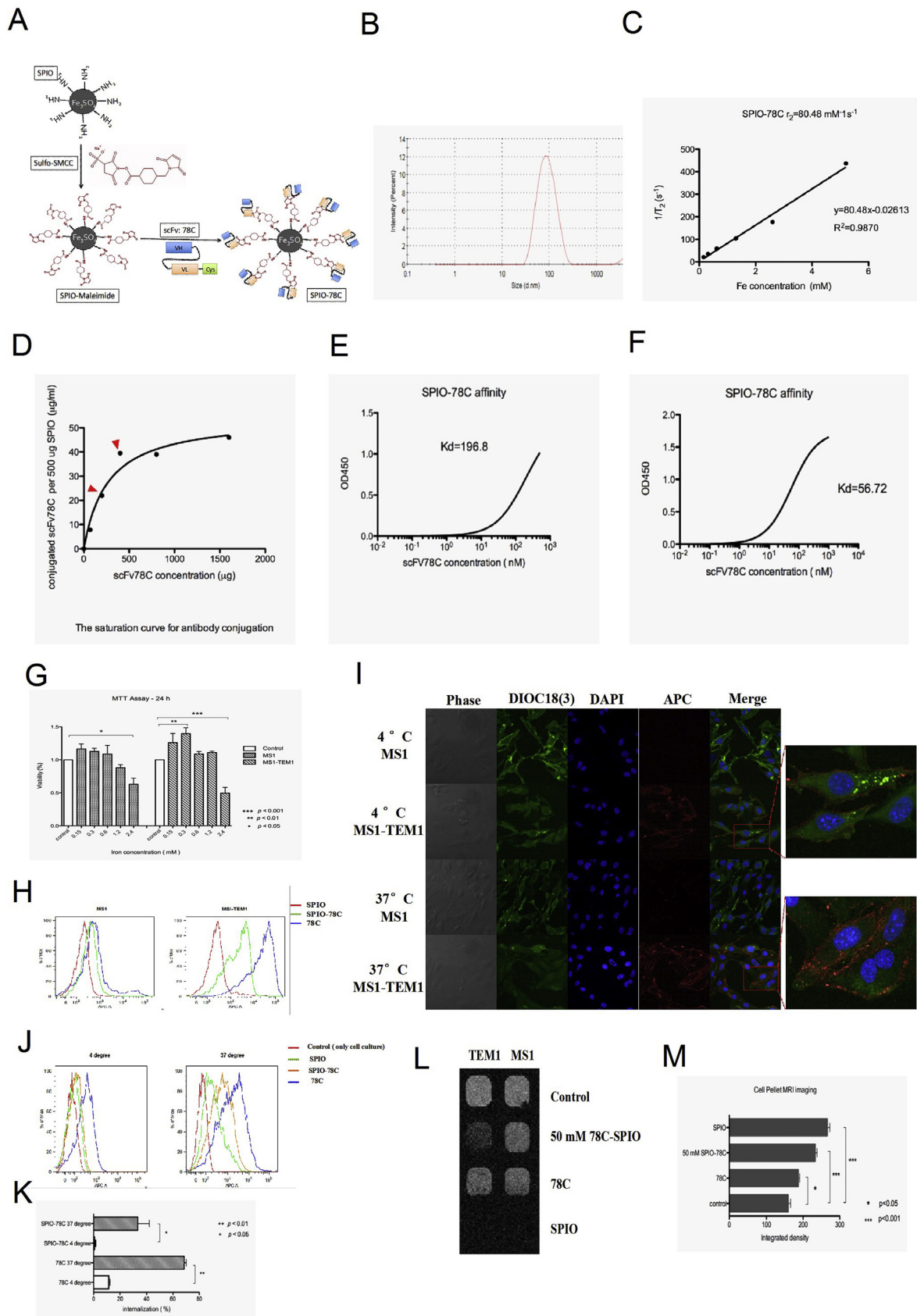
### 3.1. Construction and characterization of the cysteine-conjugated anti-TEM1 scFv (78C)

In our strategy, the reaction between maleimide and cysteine was used for the conjugation of the scFv. One free cysteine was added to the C-terminus of the scFv by adding a TCG codon (codon for cysteine) before the stop codon in the scFv cDNA sequence by PCR. The cysteine-containing scFv (78C) was purified from the *E. coli* protein expression system. One difficulty encountered when using the modified scFv purification method was inclusion body formation because of the cysteine introduction. According to the paper by Backmann et al. (2005) [7], approximately 0.5 mg of purified scFv could be obtained from a 1 L bacterial culture using immobilized metal ion affinity chromatography, while our denaturation and refolding method, which did not utilize special equipment, could produce more than 1 mg of purified scFv from a maximum of 500 ml of bacterial culture, and the final concentration of the modified scFv ranged from 1–1.8 mg/ml. The purity of 78C was determined by SDS-PAGE, and the affinity was tested by ELISA. The results demonstrated that more than 95% purity for the modified scFv could be obtained by our purification procedure (Fig. 2A), and the modified scFv had very high affinity (3.94 nM) (Fig. 2B).

### 3.2. Construction and evaluation of the nanoparticle-conjugated scFv (78C-SPIO)

Noninvasive MRI has been a very important method used for cancer diagnosis. Superparamagnetic iron oxide (SPIO) nanoparticles are the most commonly studied MRI contrast agents [11,12] and can be visualized with T2 MRI sequences as hypointense signals (dark, with negative contrast enhancement) [12]. To increase the diagnostic accuracy, the conjugation of SPIO to tumor-specific ligands, including scFv, mAbs, peptides, and even therapeutic compounds has been used. scFvs should be ideal candidates for conjugation to targeted SPIO nanoparticles due to their high affinity for antigen and reduced immunogenicity compared to mAbs. In our conjugation strategy, scFv with an introduced cysteine was used for conjugation with SPIO-maleimide. SPIO-amine was synthesized according to the protocol and then simply mixed with a small linker (sulfo-SMCC) at room temperature for 30 min to generate SPIO-maleimide. After removing the excess cross-linker, SPIO-scFv (78C-SPIO) was obtained by the incubation of scFv-cysteine (78C) with SPIO-maleimide at room temperature for 2 h or at 4 °C overnight (Fig. 3A). The SPIO diameter was approximately 80 nm (Fig. 3B), and  $r_2$  was equal to 80.48 nM<sup>-1</sup>s<sup>-1</sup> (Fig. 3C). The saturation curve for scFv conjugation was analyzed by conjugating increasing concentrations of 78C with a constant concentration of SPIO. These results demonstrated that the saturation level was reached when the concentration of 78C as higher than 400 µg (Fig. 3D). After 200 µg of 78C was conjugated with 500 µg of SPIO, the exact scFv concentration in the presence of SPIO was only 22 µg/ml. The affinity of 78C-SPIO in this conjugation condition was 196.8 nM, as measured by ELISA (Fig. 3E). After 400 µg of 78C was conjugated with 500 µg of SPIO, the exact scFv concentration in the presence of SPIO was 39 µg/ml, and the affinity was 56.72 nM (Fig. 3F). Based on these results, the conjugation concentration ratio used for SPIO and 78C was 500 µg to 400 µg for the subsequent experiments. SPIO can be cytotoxic. Therefore, the cytotoxicity of SPIO-78C in MS1 and MS1-TEM1 cells was assessed using an MTT assay. Cells were incubated with SPIO-78C with equivalent concentrations of iron ranging from 0.15 to 2.4 mM for 24 h. Based on previous results, the cell viability should have been decreased when the concentration of iron reached 1.2 mM. However, significantly decreased cell viability was observed only when the concentration reached 2.4 mM (Fig. 3G).

The specificity of SPIO-78C was evaluated by flow cytometry. Compared to 78C alone, decreased specificity was observed, indicating



(caption on next page)

**Fig. 3.** Construction and evaluation of the nanoparticle-conjugated scFv (78C-SPIO). **A.** The scheme of SPIO conjugation to 78C scFv. The conjugation of 78C scFv antibody (containing free Cys) to maleimide functionalized SPIO **B.** SPIO diameter. **C.** Calibration curve of iron concentration versus relaxation rate. **D-F.** The saturation curve for antibody conjugation was analyzed by conjugating increasing concentrations of scFV78C to a constant concentration of SPIO (500  $\mu\text{g}$ ). The affinity for the 22  $\mu\text{g}/\text{ml}$  SPIO-78C (After 200  $\mu\text{g}$  78C conjugating with 500  $\mu\text{g}$  SPIO, the accurate scFV concentration on the SPIO is 22  $\mu\text{g}/\text{ml}$ ) and the 39  $\mu\text{g}/\text{ml}$  SPIO-78C (After 400  $\mu\text{g}$  78C conjugating with 500  $\mu\text{g}$  SPIO, the accurate scFV concentration on the SPIO is 0.39  $\mu\text{g}/\text{ml}$ ) is 196.8 nM and 56.72 nM, respectively. **G.** In vitro assessment of cytotoxicity of SPIO-78C in MS1 and MS1-TEM1 cells by MTT assay. The cells were incubated with SPIO-78C at equivalent iron concentration ranging from 0.15 to 2.4 mM for 24 h. And the results was detected and the statistical analysis by one way ANOVA test and Tukey's multiple comparison. ( $n = 3$ ). **H.** Flow cytometric analysis for SPIO-78C specificity in MS1 or MS1-TEM1 cell. The cells were incubated with SPIO, 78C or SPIO-78C at 4  $^{\circ}\text{C}$  for 2 h. Both concentration for 78C and SPIO-78C are 50 mM. **I.** Confocal for SPIO-78C internalization in MS1 or MS1-TEM1 cell. The cells were incubated SPIO-78C at 4  $^{\circ}\text{C}$  or 37  $^{\circ}\text{C}$  for 2 h. The concentration for SPIO-78C is 50 mM. **J-K.** Flow cytometric analysis for SPIO-78C internalization in MS1-TEM1 cell. The cells were incubated with SPIO, 78C or SPIO-78C at 4  $^{\circ}\text{C}$  or 37  $^{\circ}\text{C}$  for 2 h. Both concentration for 78C and SPIO-78C are 50 mM. The statistical analysis based on flow cytometric results was conducted by one way ANOVA test and Tukey's multiple comparison test. ( $n = 2$ ). **L-M.** MRI results was detected and the statistical analysis by one way ANOVA test and Tukey's multiple comparison. ( $n = 2$ ).

that the SPIO conjugation procedure or SPIO itself affected the specificity of the scFv. However, compared to the control group, a significant peak shift was still observed in the SPIO-78C group, indicating that SPIO-conjugated scFv retained a high level of antigen-specific binding (Fig. 3H). Confocal microscopy was also used to characterize the 78C-SPIO (Fig. 3I). Compared to the results for the TEM1-negative cells in both the 4  $^{\circ}\text{C}$  and 37  $^{\circ}\text{C}$  groups, 78C-SPIO specifically bound to the TEM1-positive cells. One important biological function of scFvs are their internalization ability. After scFvs specific bind with the antigen in vivo, the bound complex will enter cells, which is very important for the accumulation of the probe in the cell and will ultimately influence the imaging efficiency. Based on the confocal data, the location of 78C-SPIO (red) was completely different in the TEM1-positive group when the cells were incubated at different temperatures. 78C-SPIO was found inside the cells at a high density in the 37  $^{\circ}\text{C}$  group and was only found on the cell membrane at a very low density in the 4  $^{\circ}\text{C}$  group. This indicated that even after conjugation with 80 nm SPIO, the internalization ability of 78C-SPIO remained high. To further confirm the internalization ability, flow cytometry was used. Compared to that in the 4  $^{\circ}\text{C}$  group, the peak of 78C-SPIO in the 37  $^{\circ}\text{C}$  group was dramatically shifted, indicating that the internalization ability of 78C-SPIO remained high. However, compared to the 78C group, less internalization ability was found mainly due to SPIO (Fig. 3J). Statistical analysis with one-way ANOVA and Tukey's multiple comparison tests confirmed this conclusion (Fig. 3K). However, we believe there should be no dramatic effect of 78C-SPIO during MRI testing because of this small change in the specificity and internalization ability after the SPIO conjugation procedure. To confirm this hypothesis, cell pellet MRI was used. Unlabeled SPIO showed strong positive results, while the control group and the 78C alone group, which had no SPIO, showed negative results. Compared to the TEM1-negative group, 78C-SPIO showed TEM1-specific binding with significant MRI density (Fig. 3L and M).

In sum, these results demonstrated that our strategies for SPIO conjugation with scFv resulted in few effects on affinity, specificity and internalization ability. Moreover, strong antigen-specific MRI density was obtained with 78C-SPIO.

### 3.3. Construction and evaluation of the fluorescent dye-conjugated scFv (78C-ICG)

Optical molecular imaging is an important method of molecular imaging. Infrared radiation is light with a wavelength between 780 nm and 100  $\mu\text{m}$  and has very high permeability and safety compared to that of ultraviolet radiation. This makes it perfect for use with optical imaging dyes. Indocyanine green (ICG) is one of the infrared-irradiating dyes that has been FDA approved and is widely used for clinical examinations. Moreover, in addition to its use in diagnosis, it has also been used in cancer immunotherapy due to its phototherapy. We used ICG to test the feasibility of the use of our strategies for scFv conjugation to a fluorescence probe. ICG-maleimide was obtained simply by conjugating ICG-NHS to MAL-PEG-NH<sub>2</sub> for 2 h at room temperature. 78C-ICG was obtained by the conjugation of ICG-maleimide and scFv-

cysteine via the reaction between maleimide and cysteine (Fig. 4A). After the purification of 78C-ICG, the affinity of the conjugated scFv was evaluated by ELISA. Our results showed that the affinity of the probe-conjugated scFv (78C-ICG) was 8.091 nM, and the conjugation procedure had little effect on the affinity upon comparison with the affinity of the original scFv (Fig. 4B). The specificity was also evaluated by flow cytometry. Compared to that in TEM1-negative cells (MS1), the peak of 78C-ICG was dramatically shifted in the TEM1-positive cells (MS1-TEM1), which indicated that the specificity of the ICG-conjugated scFv was still very high. However, compared to that of the unconjugated scFv 78C, there was little effect on the TEM1 targeting efficiency, which was probably due to the conjugation procedure. Moreover, compared to that in the control group or the ICG only group, in the TEM1-negative cell group, the 78C-ICG group also had a peak shift (Fig. 4C). We believe this was due to the high concentration of 78C-ICG used in the experiment (50 nM).

We used a linker in our conjugation strategy for small-sized fluorescence dyes to avoid the disruption of the HVR by the dye. To confirm the importance of the linker, the affinity of 78C-ICG with a linker and 78C-ICG without a linker was tested by optical imaging. According to the results, a nonspecific reaction was found in the TEM1-negative cell group when the concentration was equal to or higher than 33.3 nM. A specific reaction was found at a concentration ranging from 11.1 nM to 1.2 nM. However, in comparison to that of 78C-ICG without a linker, increased fluorescence density was found in the group with 78C-ICG with a linker, which indicated the increased affinity of 78C-ICG with a linker compared to that of 78C-ICG without a linker (Fig. 4D). To explain the above described results, SDS-PAGE with native gels was used to analyze the differences in protein structure after the conjugation of ICG with and without a linker. Based on the results, compared with the linker group, many more protein bands were observed in the group without a linker (Fig. 4E).

Internalization ability is very important for scFv-based diagnosis and immunotherapy. The stronger the internalization ability is, the greater the amount of probe that will remain in the tumor. The internalization ability of 78C-ICG was measured by flow cytometry. After incubation with MS1 or MS1-TEM1 cells at 37  $^{\circ}\text{C}$  or 4  $^{\circ}\text{C}$ , the 78C-ICG group or the control groups were treated with trypsin to remove all of the surface probes. The results demonstrated that a dramatic peak shift was found in the 78C-ICG group incubated at 37  $^{\circ}\text{C}$ , and this phenomenon could be avoided by changing the incubation temperature to 4  $^{\circ}\text{C}$  (Fig. 4F). These results indicated that internalization was a biological process, and our conjugation methods could preserve this ability even after the scFv was conjugated to the probe and the linker. However, compared to that of 78C alone, the internalization of 78C-ICG was slightly decreased due to the conjugation method used (Fig. 4G).

## 4. Discussion

Antigen-specific reactions via scFv-based "molecular imaging" will become more important for the diagnosis and even immunotherapy of tumors. The development of strategies for the conjugation of a probe

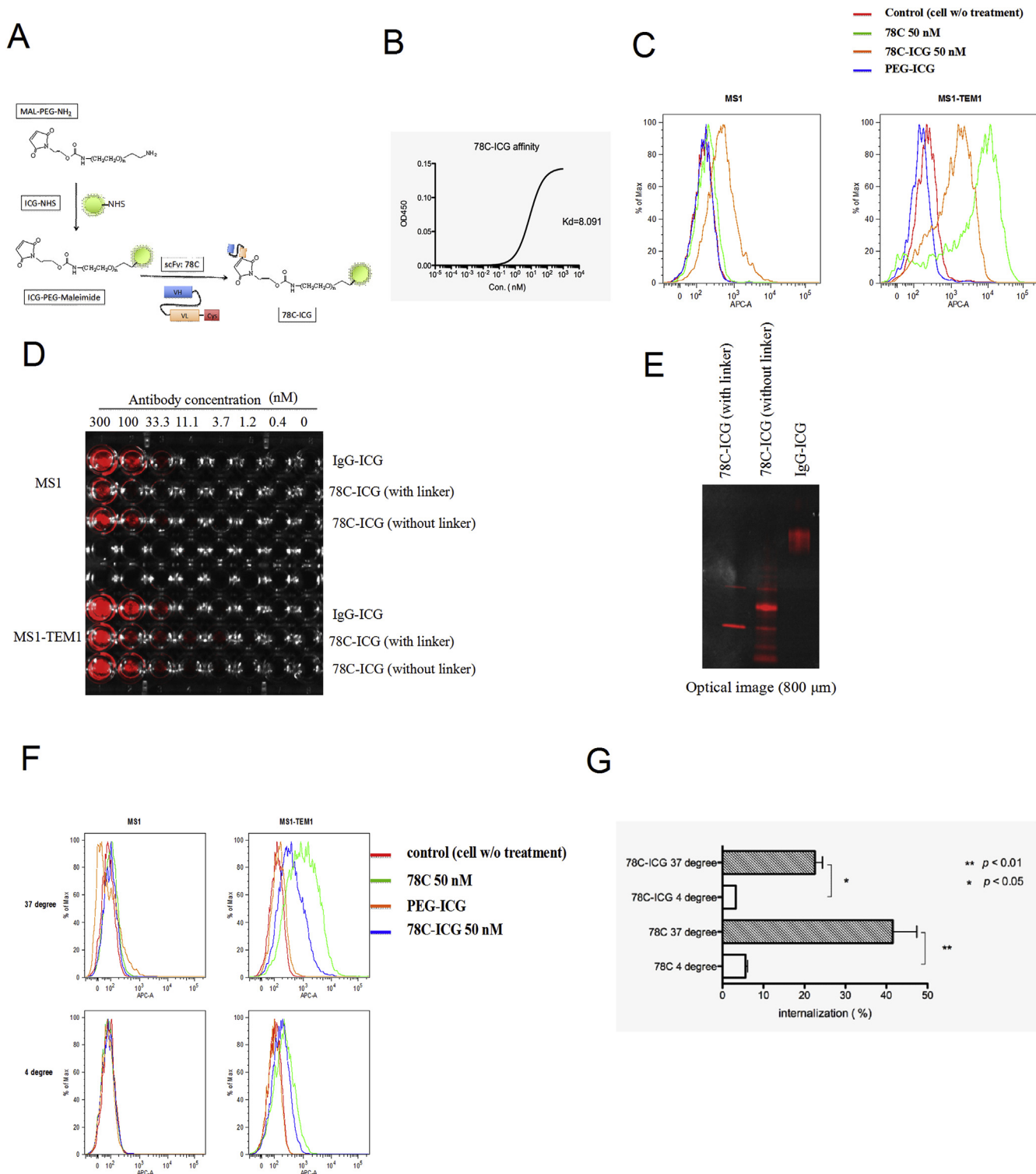


**Fig. 4.** Construction and evaluation of the ICG-conjugated scFv (78C-ICG). **A.** The scheme of ICG conjugation to 78C scFv. functionalization of MAL-PEG-NH<sub>2</sub> with ICG-NHS react first, and then conjugation of 78C scFv antibody (containing free Cys) to maleimide functionalized ICG. **B.** The affinity of 78C-ICG was detected by cell-ELISA. **C.** The specificity of 78C-ICG was detected by flow cytometry. **D.** The cell affinity of 78C-ICG was detected based on fluorescence density. **E.** The native SDS-PAGE was detected based on the fluorescence density **F-G.** 78C-ICG internalization in MS1-TEM1 or MS1 cell was detected by flow cytometry the statistical analysis by one way ANOVA test and Tukey's multiple comparison. (n = 3).

and an scFv that do not change the characteristics of the scFv are very important. The feasibility of our simple strategy has been demonstrated by all the reported results. After conjugation with SPIO or ICG via a linker, the scFv still retained high affinity, antigen specificity, and strong internalization ability. The application of these conjugated

probes was also confirmed by optical imaging and MRI. ICG conjugation methods are used in many different types of research. Many methods simply involve adding ICG to the antibody or protein without a linker [13,14], but a linker was used in our strategy. As the antigen was directly combined with the highly variable region (HVR) of the scFv,

the overall stability of the structure of the HVR is very important for the specific reaction between the antigen and the scFv. We believed that without a linker, ICG could be conjugated to the NH<sub>2</sub> residues in the scFv, which could affect the structural stability of the scFv and thereby decrease the specificity of the antibody. And we believed the same advantage of the linker should be also benefit for MRI probe.

Noninvasive MRI has been a very important method used for cancer diagnosis. SPIO nanoparticles are the most commonly studied MRI contrast agents and these nanoparticle surfaces always had been modified with functional groups such as dextran, heparin, dimercaptosuccinic acid or the net charges of SPIO nanoparticles. However, it has been reported that these groups on SPIO can markedly influence the internalization of SPIO nanoparticles [15]. Therefore, in our conjugation strategy, scFv with an introduced cysteine was used for conjugation with SPIO-maleimide. SPIO-amine was synthesized according to the protocol and then simply mixed with a small linker (sulfo-SMCC) at room temperature for 30 min to generate SPIO-maleimide. This strategy still could retained high internalization of SPIO nanoparticles.

The methods used to implement this strategy were also very simple. The cysteine can be added by normal PCR, and the modified scFv can be purified by an *E. coli* expression system, which is the most common type of protein purification system used in biological labs. Moreover, no special conditions were needed for any of the incubation or conjugation steps. In conclusion, we believe that our simple strategy paves the way for the construction of scFv-conjugated MRI or fluorescence probes with high affinity, strong specificity and internalization ability for cancer diagnosis or even immunotherapy.

#### Ethical approval and consent to participate

No human samples or animal experiments were conducted in this study.

#### Consent to publish

All of the authors consent to the publication of this manuscript.

#### Availability of data and materials

All the data related to this paper have been submitted to the journal.

#### Declaration of competing interest

The authors declare no conflicts of interest.

#### Acknowledgments

XC conducted the experiments and analyzed the data; CX

participated in the experimental design; YM, YX and LG participated in the data analysis; ZA and BH supervised and participated in the data analysis and interpretation and the writing of the manuscript. All authors read and approved the final manuscript. This work was supported by the Tianjin Municipal Commission of Education (11601502/19KJ01010093).

#### Appendix A. Supplementary data

Supplementary data to this article can be found online at <https://doi.org/10.1016/j.lfs.2019.117052>.

#### References

- [1] F. Ochsenbein, P. Klenerman, U. Karrer, et al., Immune surveillance against a solid tumor fails because of immunological ignorance, *Proc. Natl. Acad. Sci. U.S.A.* 96 (5) (1999) 2233–2238.
- [2] M.T. Spiotto, P. Yu, D.A. Rowley, et al., Increasing tumor antigen expression overcomes “ignorance” to solid tumors via crosspresentation by bone marrow-derived stromal cells, *Immunity* 17 (6) (2002) 737–747.
- [3] D. Colcher, G. Pavlinkova, G. Beresford, et al., Pharmacokinetics and biodistribution of genetically-engineered antibodies, *Q. J. Nucl. Med.* 42 (1998) 225–241.
- [4] F. Kampmeier, et al., Rapid optical imaging of EGF receptor expression with a single-chain antibody SNAP-tag fusion protein, *Eur. J. Nucl. Med. Mol. Imaging* 37 (2010) 1926–1934.
- [5] G. Pavlinkova, G.W. Beresford, B.J. Booth, et al., Pharmacokinetics and biodistribution of engineered single-chain antibody constructs of MAb CC49 in colon carcinoma xenografts, *J. Nucl. Med.* 40 (1999) 1536–1546.
- [6] T. Yokota, D.E. Milenic, M. Whitlow, et al., Rapid tumor penetration of a single-chain Fv and comparison with other immunoglobulin forms, *Cancer Res.* 52 (1992) 3402–3408.
- [7] Natalija Backmann, Christian Zahnd, Francois Huber, et al., A label-free immunosensor array using single-chain antibody fragments, *Proc. Natl. Acad. Sci.* 102 (41) (2005) 14587–14589.
- [8] J. Hunn, G.C. Rodriguez, Ovarian cancer: etiology, risk factors, and epidemiology, *Clin Obstet Gynecol* 55 (2012) 3–24.
- [9] A. Zhao, S. Nunez-Cruz, C. Li, et al., Rapid isolation of high-affinity human antibodies against the tumor vascular marker endosialin/TEM1, using a paired yeast-display/secretory scFv library platform, *J. Immunol. Methods* 363 (2) (2011) 221–232.
- [10] Xiaopeng Yuan1, Mingjuan Yang, Xiang Chen, et al., Characterization of the first fully human anti-TEM1 scFvin models of solid tumor imaging and immunotoxin-based therapy, *Cancer Immunol. Immunother.* 66 (2017) 367–378.
- [11] D.L.J. Thorek, A.K. Chen, J. Czupryna, et al., Superparamagnetic iron oxide nanoparticle probes for molecular imaging, *Ann. Biomed. Eng.* 34 (1) (2006) 23–38.
- [12] J. Lodhia, G. Mandarano, N. Ferris, et al., Development and use of iron oxide nanoparticles (Part 1): synthesis of iron oxide nanoparticles for MRI, *Biomed. Imaging Interv. J.* 6 (2) (2010) e12.
- [13] D. Pan, S.D. Caruthers, G. Hu, et al., Ligand-directed nanobialys as theranostic agent for drug delivery and manganese-based magnetic resonance imaging of vascular targets, *J. Am. Chem. Soc.* (2008), <https://doi.org/10.1021/ja801482d>.
- [14] A. Villanueva, M. Cañete, A.G. Roca, et al., The influence of surface functionalization on the enhanced internalization of magnetic nanoparticles in cancer cells, *Nanotechnology* 20 (11) (2009) 115103.
- [15] C. Corot, P. Robert, J. Idee, et al., Recent advances in iron oxide nanocrystal technology for medical imaging, *Adv. Drug Deliv. Rev.* 58 (14) (2006) 1471–1504.